CHAPTER 7

Waveguide writing in optimal conditions

7.1 Introduction

In this chapter, we want to emphasize the technological interest of controlled laser-processing in dielectric materials. Since the first report of femtosecond laser induced refractive index modification in the bulk of glass by Davis et al. [115], a plethora of technological applications employing ultrashort laser pulses to process the bulk of transparent materials emerged. Direct writing of Fresnel lenses [77] , data storage elements [116], couplers, diffraction gratings [117], beam splitters, and micro mirrors [118], or microfluidic devices [119] have been reported. By far, the application which has received most of the experimental effort is direct writing of embedded guiding structures. Optical waveguides have been fabricated in fused silica [115], borosilicate glasses, phosphate glasses [120], heavy metal oxide glasses [76], poly(methyl acrylate) [121], Ti^{3+}:Sa [122] among others. There are many reasons for this massive interest. Firstly, waveguide writing in crystals like Ti^{3+}:Sa offers an alternative to photolithographic processes for the fabrication of innovative light sources [122]. Then, combined to etching techniques, microfluidic devices can be designed [119], with a promising future in lab-on chip devices [123]. Telecommunication applications are also concerned, as fabrication of low-loss waveguides and splitters have been demonstrated at telecommunication wavelengths (1310 and 1550 nm) [124]. Femtosecond written arrays of waveguides have also been used to study the behavior of discrete solitons [125].

Therefore, we now attempt to demonstrate that laser-writing of waveguides in BK7 is possible, as a proof of principle. BK7 is particularly interesting for several purposes. At first,

no low-losses optical waveguides could be imprinted in this glass. Secondly, Schott BK7 glass is the most common borosilicate crown glass used for commercial optics (lenses, windows, mechanical substrates). In this way, we want to illustrate that a good understanding of the basic processes combined with adequate laser processing methods and post-irradiation diagnosis constitutes a solid basis for developing non conventional, flexible, and viable fabrication techniques.

We are aware that waveguide writing is a delicate task, and that a specific equipment (in particular regarding motors and vibration free environment) as well as suitable characterization techniques have to be employed. Therefore, in this chapter, the accent is put on two things. At first, in a longitudinal writing configuration, the correlation between morphology in PCM and guiding properties is established. Then, a first set of results is presented in a transverse writing configuration. Finally, we propose optimal processing conditions (pulse energy, scanning velocity, and temporal shape) for writing low losses, high refractive index channels in the bulk of BK7.

7.2 Waveguide laser-writing in longitudinal configuration

As discussed in Sec. 3.2.2, spherical aberrations have drastic consequences on the pulse peak intensity and on the beam profile when focusing deep in the bulk [4, 97]. Some estimations based on the resolution of Eq. 3.20 indicate that when writing deeper than 200 μm in the bulk, beam distortion upon spherical aberrations can not be neglected. Therefore, at the present time, longitudinal waveguide writing (LWW) can not be considered as a viable method for moderate and high NAs. In Sec. 6.4.2, temporal pulse shaping was proposed as a possible alternative for controlling the energy deposition in presence of aberrations but the application to LWW would necessitate a progressive correction. This is beyond the scope of the present work. Nevertheless, LWW offers some indisputable advantages, especially regarding the circularity of the laser-generated optical structures. In consequence, the far-field patterns observable when injecting the optical waveguides are also more circular and easier to interpret.

At first, there is a need for a correlation between aspect in PCM and guiding properties. To this extent LWW seems to be an adequate method. Both fused silica and BK7 have been studied. The corresponding PCM profiles are presented in both cases and finally, the more suitable optical structures are used for far field analysis, including a preliminary estimation of the amplitude of the laser induced refractive index change.

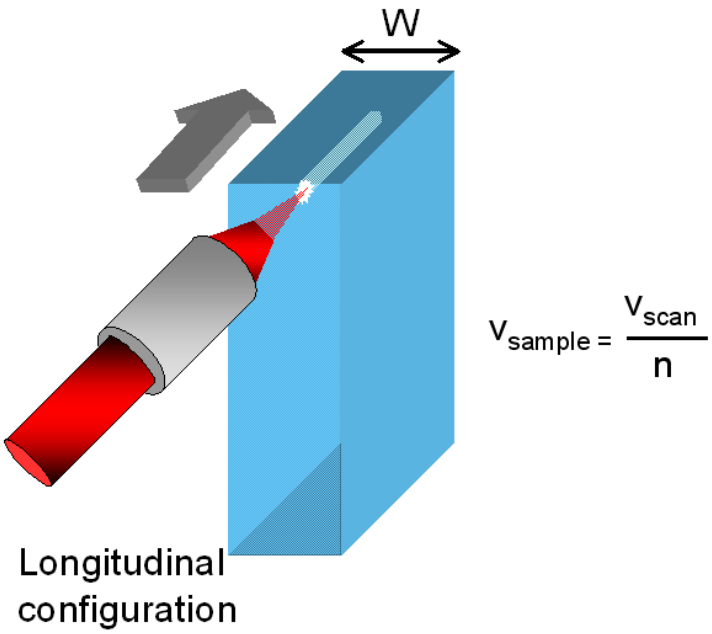

Figure 7.1: Experimental layout employed for longitudinal waveguide writing (adapted from [9]). The thickness of the sample (W) is of 5 mm in order to avoid beam clipping. Note the difference between the sample velocity V_{sample} and the velocity of the focal point V_{scan} inside the sample of refractive index n. The arrow indicates the direction of the sample movement.

7.2.1 Experimental configuration

A sketch of the experimental setup is shown in Fig. 7.1. The laser source employed is system IV, characterized by a 100 kHz repetition rate. The sample is mounted on a PI M-126.DG (Physik Instrumente). In this configuration, the velocity of the focal point V_{scan} is $\approx n$ times higher than the sample velocity V_{sample}, where n is the refractive index of the pristine bulk. The extremities of the waveguides are located at a minimum distance of 0.4 mm away from the sample surfaces, to avoid damaging. Thicker samples (W=5 mm) are used in order to avoid laser beam clipping when writing in the depth of the bulk.

The waveguides are characterized at a 633 nm wavelength provided by a He-Ne laser source. The injection was made with the microscope objective as we used for generating the optical structure. The analysis presented in Sec. 7.2.3 is based on a recording of the far-field pattern in a plane located 115 cm far from the waveguide output with a commercially available digital camera.

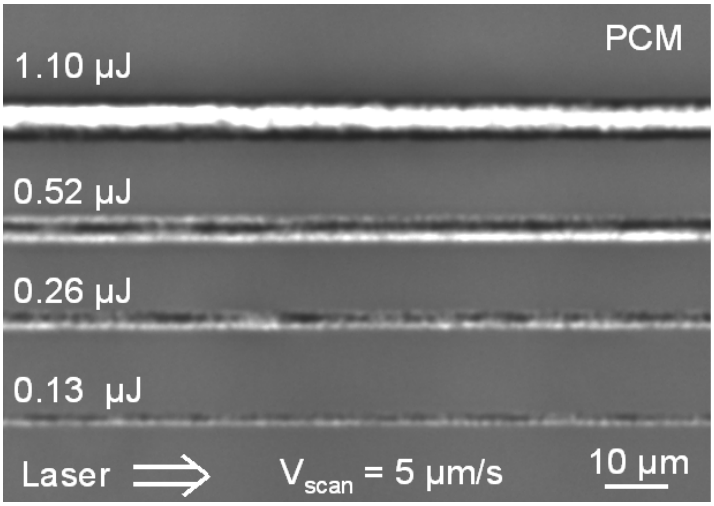

Figure 7.2: Phase-contrast microscopy observation of an array of optical structures written longitudinally in a-SiO_2. The laser energy is indicated in microjoules. The scan speed is of 5 μm/s. The laser source employed has a repetition rate of 100 kHz.

7.2.2 Experimental conditions and phase contrast microscopy analysis

Fused silica

Although waveguide writing in fused silica has been widely demonstrated, including in longitudinal writing configurations [126, 115, 127, 128, 129, 9] we could not find reports of longitudinal waveguide writing with a numerical aperture (NA) as high as 0.45. Indeed, our investigations show that a narrow processing window only can eventually be exploited, and although no analysis were carried out in this direction, it is assumed that the optical structure written with an energy of 0.52 μJ per pulse and V_{scan} =5 μm/s visible in Fig. 7.2, may have relevant properties. In most of the cases, the laser-induced structures appear brighter than the background in PCM, probably because of scattering from the light source. Nevertheless we could not detect the waveguides in OTM, indicating that we are not in an interaction regime inducing sample damage.

BK7

In the same way, we attempted to find favorable conditions to imprint a guiding structure in BK7 in a longitudinal writing configuration. We could find a relevant set of parameters, providing a dark and smooth structure in PCM, hardly visible in OTM. It appears that this type of structure can be generated exclusively when the laser energy exceeds 0.8 μJ per

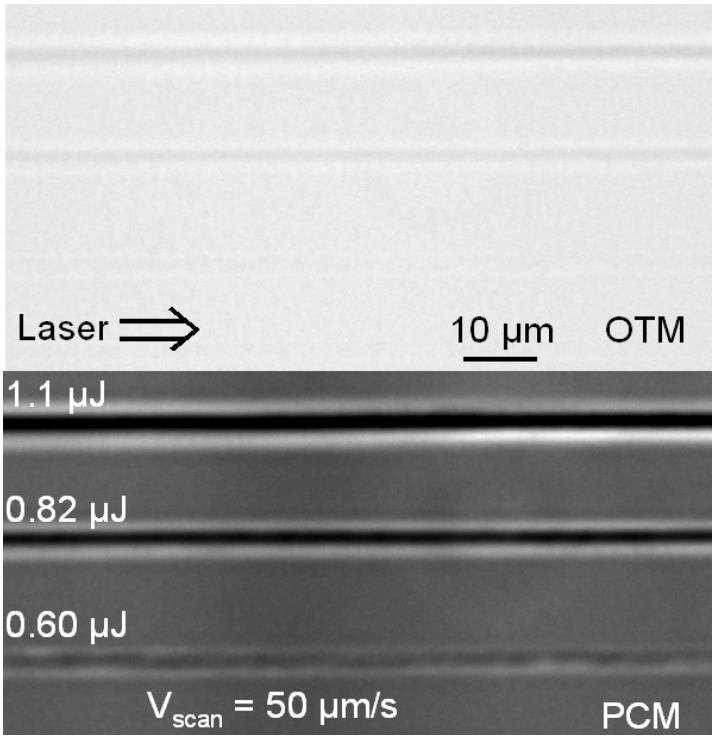

Figure 7.3: Optical transmission microscopy (OTM) and phase-contrast microscopy (PCM) observations of an array of optical structures written longitudinally in BK7 with a 150 fs pulse duration. The laser pulse energy is indicated in microjoules. The scan speed is of 50 μm/s. The laser source employed has a repetition rate of 100 kHz. The contrast of the OTM picture was uniformly enhanced in order to render the structures visible.

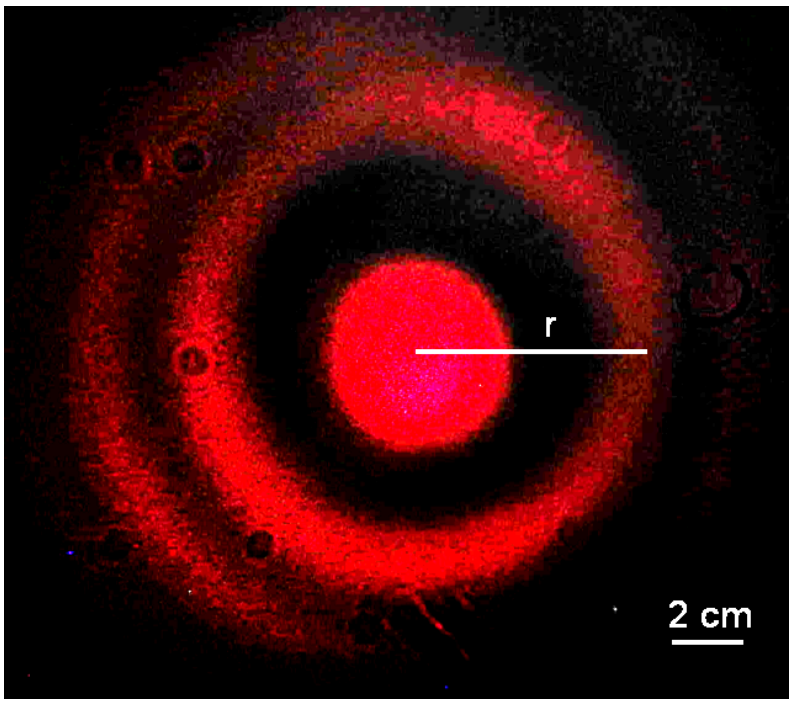

Figure 7.4: Intensity distribution in a plane located at 115 cm far from the exit of a waveguide written longitudinally in BK7 with a laser energy of 1.1 μJ and a pulse duration of 130 fs. The waveguide was injected with a HeNe laser through the same objective as we used for generating the structure (NA = 0.45). The radius at which the rings vanish (r) is indicated.

pulse. This laser energy corresponds to a regime where a black shell appears in the periphery of the irradiated region (See Fig. 4.10).

Because of the spherical aberrations, the peak power drops with the writing depth. As a consequence, the dark and smooth structures progressively vanish at a depth comprised between 2 and 3 mm into the bulk.

7.2.3 Analysis of the guiding properties in far field

In fused silica, the PCM analysis did not show the expected characteristics of a good waveguide, i.e. a strong positive refractive index change and a transparent profile in OTM, except maybe for the structure corresponding to a laser pulse energy of 0.52 μJ in Fig. 7.2. Therefore, we concentrated our efforts on structures written in BK7.

Presentation of the far field pattern

The optical structure corresponding to a laser pulse energy of 1.1 μJ in Fig. 7.3 was injected. The corresponding far field pattern is presented in Fig. 7.4. The distribution of intensity in

far field exhibits concentric rings, interpreted as an interference pattern between the different guided modes [128] or as an interference phenomenon between the coupled and uncoupled light from the He-Ne [127].

Estimation of the numerical aperture and of the laser-induced refractive index change

Based on the analysis of the far field pattern, a quantitative estimation of the numerical aperture (NA) of the waveguide can be performed according to [127]

$$NA = \sin\left(\arctan\left(\frac{r}{D}\right)\right), \tag{7.1}$$

where D is the distance between the waveguide exit plane and the plane where the far field pattern is recorded, and r is the radius at which the rings fade away. In absence of an objective criterion, it is difficult to assign a value to r. As the second outer ring is not fully visible, r was associated to the radius of the first ring, resulting in a NA of 0.086. Considering that $NA = \sqrt{2n\Delta n}$ [127, 130] where n is the refractive index of the pristine bulk, the induced index change Δn is estimated at $\Delta n = 0.25 \times 10^{-2}$.

7.2.4 Conclusion

In this section, we have demonstrated that a region appearing smooth, regular and dark in PCM constitutes indeed an optical waveguide. Surprisingly, the more efficient structures have been fabricated in BK7, where no fabrication of low losses waveguiding structures have been reported yet to our knowledge. An interaction regime resulting in a smooth channel, appearing dark in PCM has been triggered, resulting in an index change of about 0.25 % .

7.3 Waveguide laser-writing in transverse configuration

Although a few disadvantages arise from transverse writing geometries, in particular regarding the ellipticity of the imprinted structures, the maximal length of the laser written structure is potentially limited by the size of the sample only. In this section, we show a PCM observation of a waveguide written in fused silica, as an example, but the emphasis is put on waveguide writing in BK7. We attempt to demonstrate the benefits of controlling the energy deposition via the temporal shape of the input pulse.

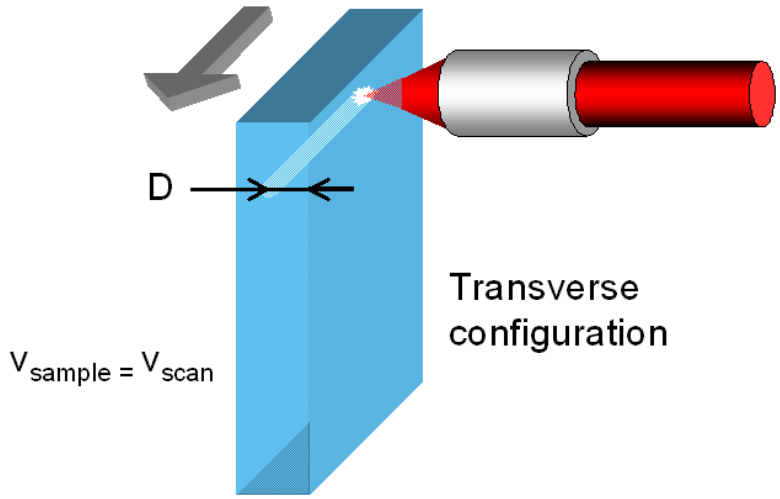

Figure 7.5: Experimental layout employed for transverse waveguide writing (adapted from [9]).The arrow indicates the direction of the sample movement.

7.3.1 Experimental configuration

A sketch of the experimental configuration is proposed in Fig. 7.5. The laser source is system IV and the sample is translated transversally with respect to the direction of the beam propagation with a motor PI M-126.DG (Physik Instrumente). In this configuration, the scan velocity (V_{scan}) coincides with the sample velocity. The extremities of the waveguides are located at a minimum distance of 0.4 mm away from the sample surfaces, to avoid surface damage. The focal plane is carefully set at a distance of D =200μm from the entrance surface, in order to minimize spherical aberrations. The characterization of the waveguide is made at a 633 nm wavelength provided by a He-Ne laser source. The injection was made with a 20x microscope objective (not shown in Fig. 7.5).

7.3.2 Phase contrast microscopy observations

Fused silica

For adequate laser energies and scanning velocities, a black stripe appears in the PCM observations. In Fig. 7.6, an example with a laser energy of 160 nJ and a scanning velocity of 100 μm/s is presented. According to the previous section, the dark stripe visible in PCM on the right side of the laser-generated structure indicates a potential interest for light guiding applications. By exploring different laser energies and scanning velocities, we tried to improve the dimensions and roughness of this region. The results did not show any noticeable improvement. We note that the profile of the laser-generated optical structure

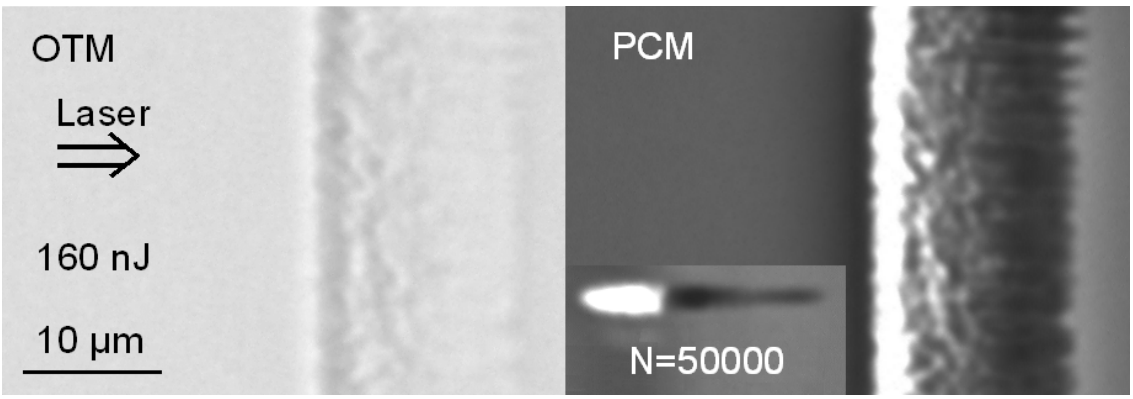

Figure 7.6: Optical transmission microscopy (OTM) and phase contrast microscopy (PCM) observations of a waveguide generated in a-SiO_2 with a laser pulse duration of 130 fs. The laser pulse energy is 160 nJ and the scan velocity is 100 μm/s. A PCM observation of the accumulation of 50000 pulses at the same laser energy is also shown.

corresponds fairly well to the profile of a single trace. To a certain extent, the waveguide can be considered as an arrangement of individual imprints written side by side, resulting in a rough final aspect.

BK7

In BK7, writing with a short pulse (SP) results in a structure hardly visible in PCM, with the behavior of a overwhelming low density, low index phase. The contrast of the low-density region appearing when writing a single trace decreases in the writing process (See Fig. 7.7 (a) and (c)). Increasing the laser energy does not bring significant improvements, as non uniform and elongated structures are generated.

Therefore, we attempted to write an optical structure using a solution provided by the evolutionary algorithm during the optimization process on the refractive index change. The temporal aspect of the input pulse (OP) was introduced in Fig. 6.12. The laser energy is the same as we used during the optimization (see Sec. 6.5.2). By translating the sample transversally with respect to the laser beam, the axial profile of the imprint is mostly conserved and a dark stripe appears in PCM, suggesting that light may be guided in this region. Contrary to what is observed in fused silica, the laser generated structure exhibits a smooth profile. The mismatch in the respective on axis extents of the imprints shown in Fig. 7.7 (b) and (d) can be explained by the different irradiation conditions. In a first approximation, $5000<N<10000$ pulses only are accumulated when a waveguide is generated at a scan speed of 100 μm/s. Secondly, the cooling dynamics are substantially altered when scanning the sample. This point is further exploited in the next section.

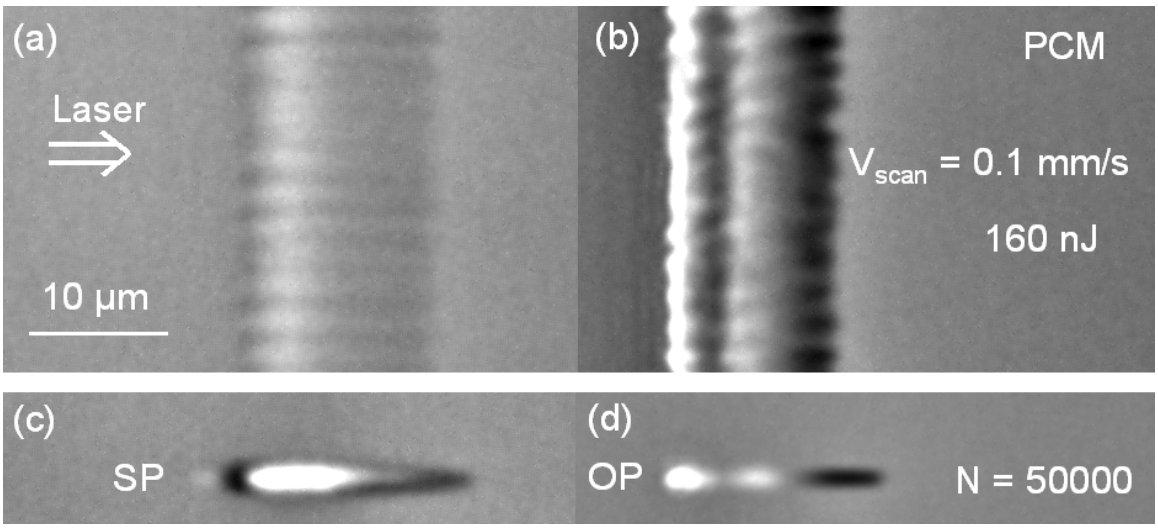

Figure 7.7: Phase contrast microscopy (PCM) observations of imprints visible in BK7 after irradiation. The structures were not visible in optical transmission microscopy. The laser energy is 160 nJ per pulse. (a): Structure generated with a femtosecond pulse duration (SP) in a transverse writing configuration. The scan velocity is of 100 μm/s. (b): Structure generated with an optimal pulse (OP) provided by the optimization algorithm. The scan velocity is of 100 μm/s. (c): Accumulated effect of N = 50000 SP. (d): Accumulated effect of N = 50000 OP.

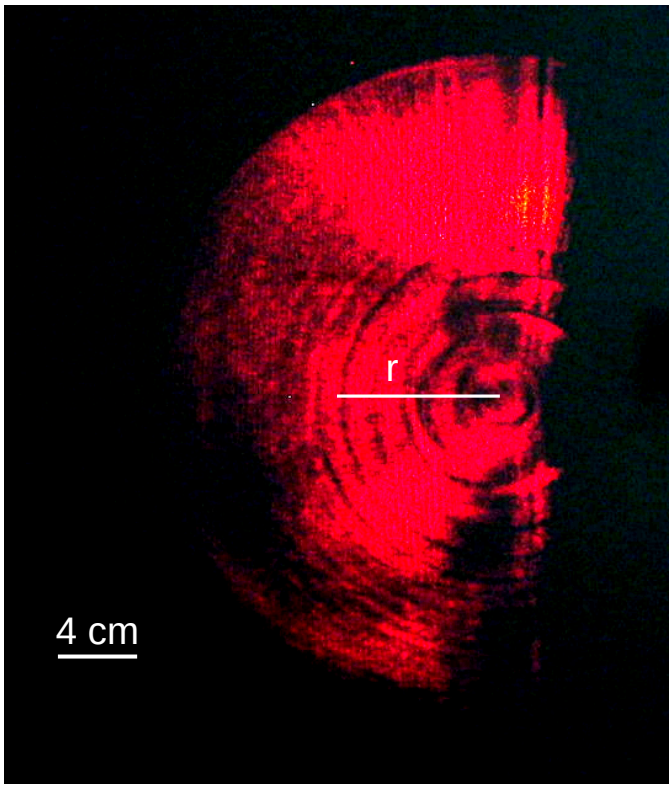

Figure 7.8: Intensity distribution in a plane located at 115 cm far from the exit of a waveguide written transversally in BK7 with a laser energy of 1.1 μm at a velocity of 100 μm/s. The waveguide was injected with a HeNe laser through a 20x objective. The radius at which the rings vanish (r) is indicated.

7.3.3 Analysis of the guiding properties in far field

Because of the sample geometry, a part of the circular far field pattern following injection by the HeNe laser is clipped. The intensity distribution in far field associated to the waveguide written in BK7 with an optimal pulse is shown in Fig. 7.8. In this case, it is delicate to perform the same type of analysis as in Sec. 7.2.3, in particular because it is difficult to assign a value to r. We finally choose r as shown in Fig. 7.8. The corresponding numerical aperture is of NA= 0.06 and $\Delta n = 0.12 \times 10^{-2}$.

7.3.4 Conclusion

We demonstrated transverse waveguide writing in BK7, using a pulse envelope provided by the optimization strategy. Nevertheless, the estimated index change is at least a factor of two smaller than in the case of longitudinal writing with high energy pulses.

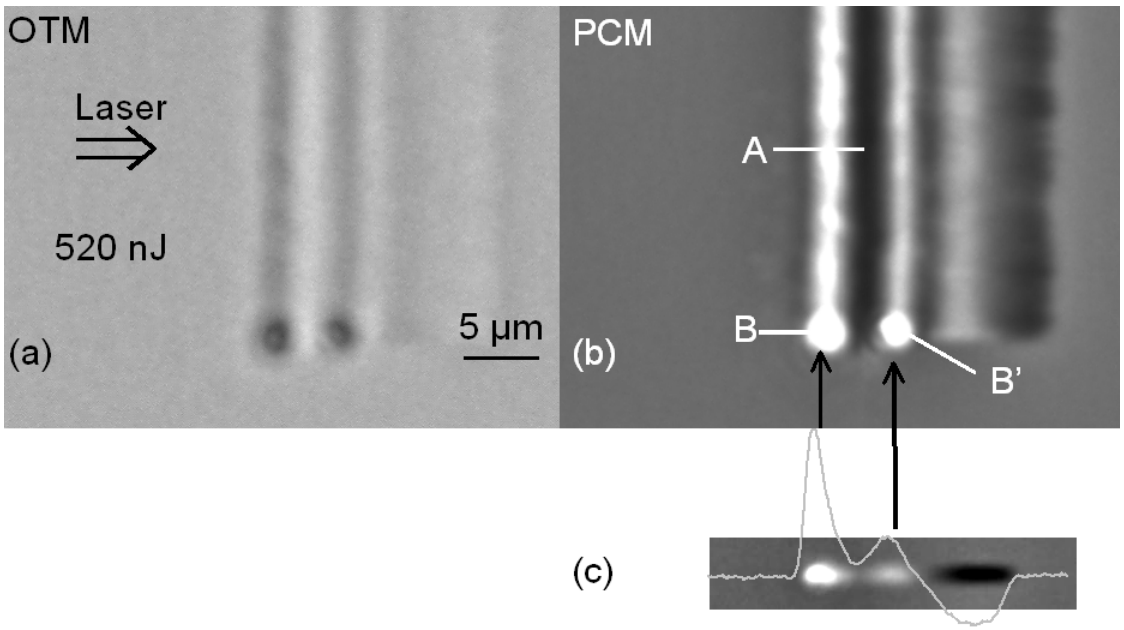

Figure 7.9: Optical transmission microscopy (OTM) (a) and phase contrast microscopy (PCM) (b) observations of imprints generated with an optimal pulse (OP) provided by the optimization algorithm in BK7. The scan velocity is of 50 μm/s. The laser energy is 520 nJ per pulse. (c): Accumulated effect of N = 50000 OP. The laser energy is 160 nJ per pulse. A gray level axial cross section is overlapped with the PCM capture.

7.4 Perspectives toward low-loss waveguiding in BK7

In search of optimal conditions for optimal structuring in BK7, several sets of processing parameters (scanning velocity, laser energy, pulse shape) were explored. As a main objective, we want to generate the same type of structure as reported in Fig. 7.3, when the laser-processing was performed longitudinally, but in a transverse writing configuration.

7.4.1 Results of preliminary investigations

It appears that using the OP obtained in Sec. 6.5.2 with the adequate laser-energy (520 nJ per pulse) generates the type of structure presented in Fig. 7.9, where the scanning velocity is of 50 μm/s. The dark stripe which was associated to the guiding part in Fig. 7.7 (b) still persists but interestingly, a channel of high refractive index (region A) with a smooth and regular appearance in PCM and invisible in OTM emerges. Region A appears as a compression zone between two moving heat sources (regions B and B'), which imprint is visible in OTM.

7.4.2 Discussion

Because the sample is being translated during the writing process and due to the presence of two heat sources, we expect the cooling dynamics in channel A to be fairly complex. According to the Fourier law, the heat flows toward the low temperatures regions, that it to say in the direction of the sample translation. A thermal expansion commences before the next laser pulse interacts with the material. When the laser energy is coupled into the bulk, the two heat sources B and B' are created and material flows away from regions B and B', creating an intricate thermoinduced stress pattern in region A. Material is confined between the two heat sources and undergoes a plastic flow. A high density material finally emerges upon cooling.

7.4.3 Future work

Those recent advances suggest that the future experimental efforts should go in two directions.

A first point to address concerns the optical properties of channel A, with a quantitative estimate of the laser induced index change with one of the methods presented in Sec. 3.3.1. Additionally, a in-depth characterization of the guiding properties (using for instance the method described in [131]) would provide a reliable and definitive indicator of the interest of those structures for waveguide writing.

Secondly, it would be highly interesting to determine whether there is a possibility to induce exclusively the heat sources B and B'. To this extent, additional optimization experiments could be very relevant.